Pol. J. Environ. Stud. Vol. 23, No. 6 (2014), 2175-2182

Original Research

Investigation of Photocatalytic Activity of C_{60}/TiO_2 Nanocomposites Produced by Evaporation Drying Method

Elżbieta Regulska, Joanna Karpińska*

Institute of Chemistry, University of Białystok, Hurtowa 1, 15-399 Białystok, Poland

Received: 22 July 2013
Accepted: 4 May 2014

Abstract

Within the last century millions of various dyes have been generated in an attempt to prepare new efficient photocatalysts for their degradation. As fullerenes are commonly known to be effective electron-donor scavengers and are very promising for synergistic reasons, fullerene-titanium dioxide (C_{60}/TiO_2) nanocomposites of different mass ratios (1:1, 1:10, 1:20, and 1:100) were prepared. Their photocatalytic properties were examined by investigating methylene blue (MB) degradation. As photodegradation of dye analysis indicated, the C_{60}/TiO_2 (1:20) composites were found to demonstrate the highest enhancement of photocatalytic activity. A series of techniques, including SEM and TEM microscopies, Raman and UV-VIS diffuse-reflectance spectroscopies, along with DSC and TGA analysis, was used to characterize the prepared material. It is expected that obtained composites will be able to create pro-ecological and cheaper methods of water disinfection, decontamination of soil, etc.

Keywords: photocatalysis, nanocomposites, TiO_2, fullerene, methylene blue photodegradation

Introduction

Because of a big demand for colored chemical compounds, more than 0.7 million tons of organic synthetic dyes are manufactured each year. They are produced mainly for use in the textile, leather goods, industrial painting, food, plastics, cosmetics, and consumer electronics sectors [1]. However, the release of colored wastewaters is considered to be a dramatic source of non-aesthetic pollution, eutrophication, and perturbations in aquatic life. Therefore, new efficient methods of their removal need to be evaluated. Among advanced oxidation processes, heterogeneous photocatalysis seems to be the most efficient. Therefore, it is commonly used in the removal of undesired substances.

It has already been applied among other dyes in the removal of malachite green [2], methylene blue [3], rhodamine B [4, 5], reactive blue [4], and titan yellow [6]. Dyes are also used as model compounds in studies concerning synthesis and/or preparation of new photocatalysts [7, 8]. Photocatalysis was also used for the degradation of other compounds. They include insecticides – imidacloprid [9]; pharmaceuticals – olanzapine [10], bezafibrate [11], sulfamethazine [3], chloramphenicol [12], anilinium [13], tetramethylammonium [4], benzoate [4], β–napthol [14], toluene [15], pentachlorophenol [16], p–toluenesulfonic acid [17], dichloroacetate [4], propanol [18], and acetaldehyde [8], as well as bacteria, e.g. *Escherichia coli* [19]. Photodegradation also has been applied in a decontamination of complex mixtures like petroleum refinery wastewater [20].

Among other semiconductors titanium dioxide (TiO_2) seems to be the most commonly used photocatalyst. However, as TiO_2 possesses a 3.2 eV energy band-gap its excitation requires ultraviolet light, which lowers the effi-

*e-mail: joasia@uwb.edu.pl

ciency of the catalytic photodegradation process. What is more, there is a need to eliminate the possibility of the electron-hole pair (e^--h^+) recombination. Therefore, different steps already have been taken toward enhancing photocatalytic activity of inorganic semiconductors. They include: dipping photocatalyst in acid solutions [21], surface chemical modification through preparation of dye-modified photocatalysts [4, 22], or by attaching other organic compounds like sulfanilic acid [23], porphyrin [24], hypocrellin B [25], metal [19], and nonmetal [26-28] doping of inorganic semiconductors and co-catalysts preparation [29].

Carbon nanostructures – TiO_2 composites constitute another group of potential photocatalysts. Different types of carbonaceous materials [30] such as carbon black [31, 32], graphite [33, 34], and graphitized materials [35, 36], have already been applied. A significant potential lies in carbonaceous nanostructures in conjunction with TiO_2 since photocatalytic activity can be attributed to the TiO_2 while the absorptivity to the fullerene. The carbonaceous-titania composites are usually obtained by sol-gel [37, 38] or evaporation-drying methods [30, 39].

The aim of our presented studies was to prepare the TiO_2-C_{60} nanocomposites and examine their photocatalytic activity. The applied evaporation-drying procedure allowed us to obtain in a short time a series of materials with varying mass ratios of C_{60} to TiO_2. Photocatalytic activity of the obtained nanocomposites was examined by investigating the methylene blue degradation in water. UV-VIS spectrophotometry was applied to monitor the bleaching of a dye. A series of techniques, including SEM and TEM microscopies, Raman and UV-VIS diffuse-reflectance spectroscopies along with DSC and TGA analysis, was used to characterize the prepared material.

Materials and Methods

Materials

TiO_2 (anatase) and methylene blue from Park Scientific Limited. HPLC-grade acetonitrile was purchased from J. T. Baker. All solutions were prepared using deionized water, which was obtained by Polwater apparatus.

C_{60}-fullerene, sublimed 99.9%, was purchased from Sigma-Aldrich, Poland

Photocatalyst Preparation

C_{60}/TiO_2 nanocomposites were prepared by evaporation-drying method as others described [39]. 2 mg of C_{60} were dispersed in deionized water and sonicated for 15 min. After that time TiO_2 powder was added and an additional 15 min of sonication were applied. The obtained suspension was heated to 80ºC in the water bath and constantly sonicated. After water evaporated, the obtained composite was dried overnight in an oven at 100ºC. C_{60}/TiO_2 nanocomposites were prepared at 1:100, 1:20, 1:10, and 1:1 mass ratios of C_{60} to TiO_2.

Characterization of the Composite

A Renishaw Raman InVia Microscope equipped with a high sensitivity ultra-low noise CCD detector was employed. The radiation from an argon ion laser (514 nm) at an incident power of 1.15 mW was used as the excitation source. Raman spectra were acquired with 3 accumulations of 10 s each, 2400 l/mm grating and using 20x objective.

Scanning electron microscopy was applied to investigate the morphology of the C_{60}/TiO_2 nanocomposites. They were imaged by secondary electron SEM with the use of an INSPECT S50 scanning electron microscope from FEI. The accelerating voltage of the electron beam was 30 keV and the working distance was 10 mm.

Differential scanning calorimetric (DSC) and thermogravimetric (TGA) analyses were performed by a Thermal Analyzer TGA/DSC 1 (METTLER TOLEDO) with a heating rate of 15ºC/min under nitrogen environment with flow rate = 20 ml/min. All runs were carried out from 25ºC to 1550ºC. The measurements were made in alumina crucibles with lids.

Photolytic as well as photocatalytic degradation experiments were carried out by irradiation with a solar simulator apparatus, namely SUNTEST CPS+ (ATLAS, USA) having energy density of 250 W/m^2.

Photocatalytic Degradation Experiment

Photocatalytic degradation experiments were performed in a 50 mL glass cell. The reaction mixture consisted of 20 mL of methylene blue (MB) sample ($6x10^{-5}$ mol/L) and a photocatalyst (1.6 mg/mL). Prior to irradiation the dye-catalyst suspension was kept in the dark with stirring for 1 hour to ensure an adsorption-desorption equilibrium. To determine MB degradation, the samples were collected at regular intervals (10 min during 1st hour and 15 min during 2nd hour) and centrifuged to remove photocatalyst.

Spectrophotometric Analysis

UV spectrophotometry was used to monitor the current concentration of MB. All spectrophotometric determinations were done using a U-2800A Hitachi spectrophotometer. The following working conditions of the apparatus were applied: scan speed 1,200 nm/min and spectral bandwidth (1.5 nm). UV studies were done using 1 cm quartz cell. Absorbance was recorded in the range of 190-700 nm, and the maximum absorption wavelength experimentally registered at λ=610 nm was used for the calibration curve and further concentration measurements.

HPLC Analysis of MB Intermediates

The chromatographic system (Thermo Separation) consisted of a 2D UV 3000 Spectra System, a P2000 low-gradient pump, a vacuum membrane degasser SCM Thermo Separation, and a Rheodyne loop injector (20 µL) were used. ChromQuest Chromatography Data system software

for Windows NT was applied for acquisition and storage of data. Waters Spherisorb ODS-2 150 mm × 4.6 mm analytical column packed with 5μm particle size was used. Separation was achieved using an isocratic method. The mobile phase consisted of an acetonitrile:water (60:40 v/v). The flow rate of the mobile phase was 1 mL/min and the injection volume was 100 μL. The column was maintained at room temperature. The DAD detector was set at 245 nm. The detected retention time of methylene blue was 2.07 min.

Results and Discussion

Characterization of C_{60}/TiO_2 Composites

The homogeneity of the obtained materials was examined. Fig. 1 shows the scanning electron micrographs of the C_{60} (Fig. 1a), TiO_2 (Fig. 1f), and C_{60}/TiO_2 composites (Figs. 1b-e). The larger flakes with a smooth surface correspond to the C_{60} while the smaller particles to the TiO_2. The proportions of smooth flakes to the smaller particles in the pre-

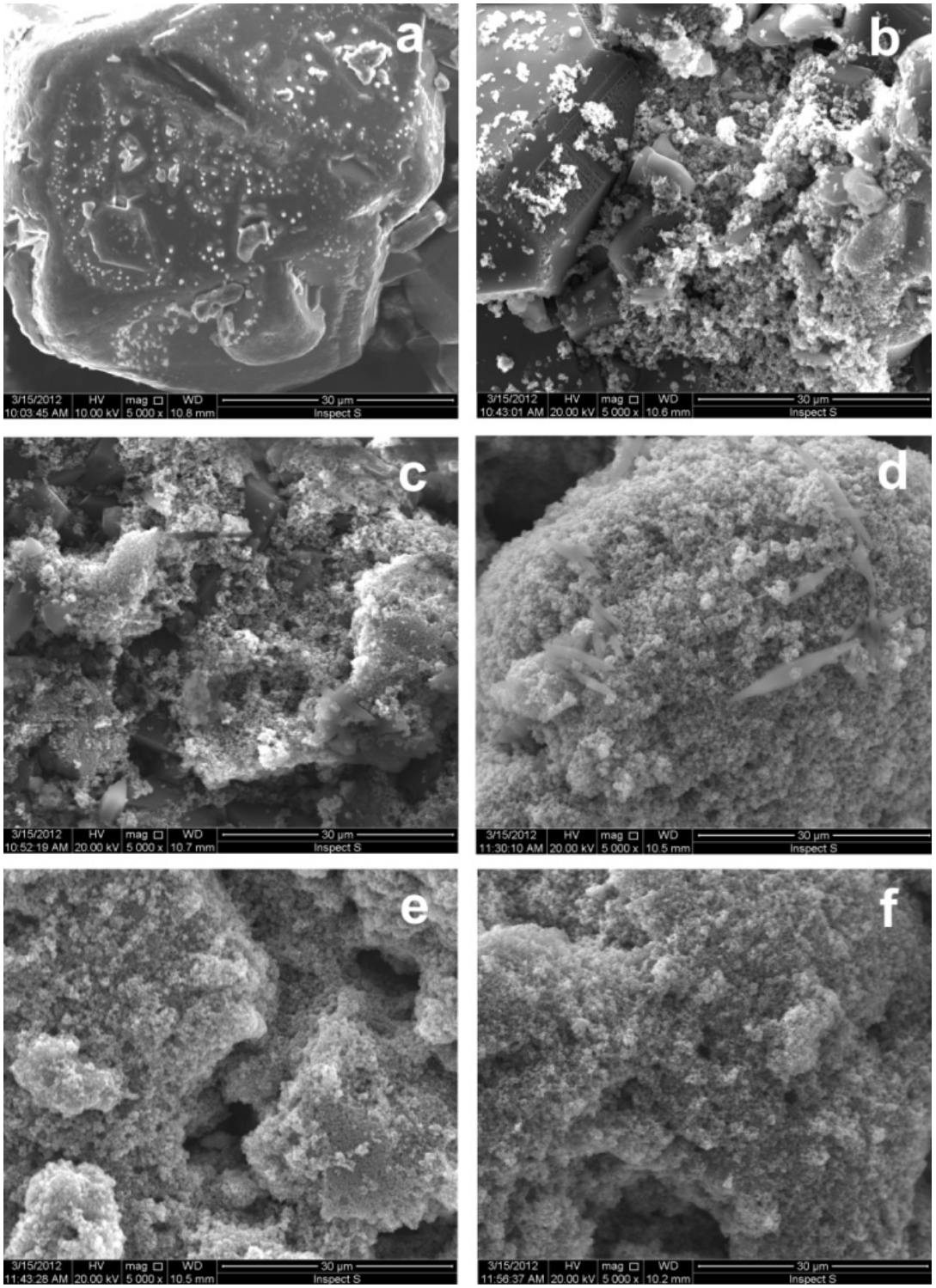

Fig. 1. SEM micrographs of C_{60} (a), C_{60}/TiO_2 (with mass ratios of 1:1 (b), 1:10 (c), 1:20 (d), 1:100 (e)) and TiO_2 (f).

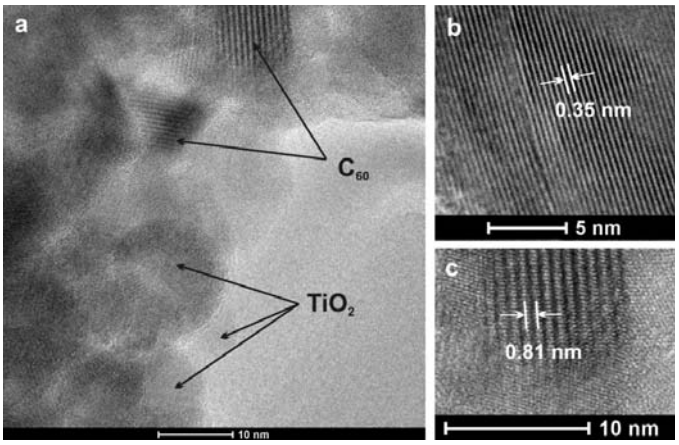

Fig. 2. TEM image of C_{60}/TiO_2 (1:20) composite (a). Magnified images of the lattice fringes coincide with the anatase form of TiO_2 (b) and fcc C_{60} crystal (c).

sented pictures is in agreement with the mass ratios of C_{60} to TiO_2 in the prepared composites. It can be seen that the greater amount of TiO_2 that was introduced, the smaller smooth surface that is present in the image. This can be attributed to the coverage of C_{60} surface by TiO_2 particles.

Transmission electron microscopy (TEM) images of C_{60}/TiO_2 (1:20) composite are presented in Fig. 2. Two sets of well-resolved lattice fringes are visible from a magnified image of Fig. 2a. The spacing of 0.35 and 0.81 nm measured for these two sets of fringes (Figs. 2b and c) coincides with the d-spacing of (011) type planes in anatase form of titania and face-center-cubic (fcc) C_{60} crystal, respectively.

The Raman spectra of the C_{60}/TiO_2 composites are illustrated in Fig. 3. In each spectrum the same number of peaks at the same Raman shifts are present. Five of them, at 142, 198, 396, 514, and 639 cm^{-1} (Fig. 2a), correspond to the anatase phase of TiO_2. They are designated as $E_{g(a)}$, $E_{g(2)}$, $B_{1g(1)}$, $A_{1g}+B_{1g(2d)}$, and $E_{g(3)}$ modes [27, 28], respectively. Those characteristic peaks of the anatase phase confirm that the TiO_2 crystal phase remained unchanged in the prepared composites. The last peak at 1,468 cm^{-1} corresponds to the pentagonal pinch mode $A_{g(2)}$ of C_{60} [29]. Above-mentioned

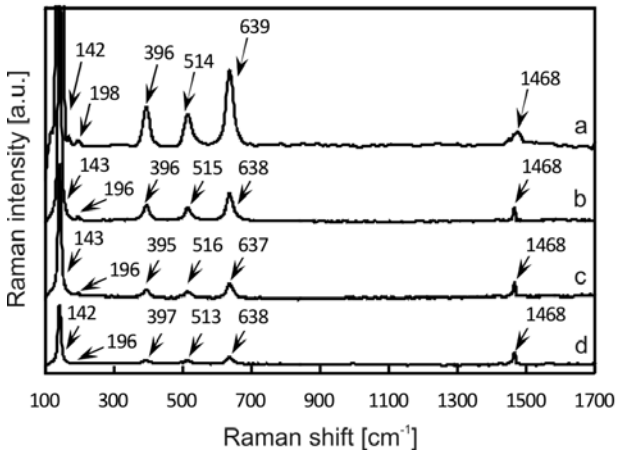

Fig. 3. Raman spectra of C_{60}/TiO_2 composites with mass ratios of 1:100 (a), 1:20 (b), 1:10 (c), 1:1 (d).

spectra indicate the presence of both components of the C_{60}/TiO_2 nanocomposite.

Thermal profile of prepared composites was obtained by thermogravimetric (TGA) and differential scanning calorimetric (DSC) analysis. TGA curves of C_{60}/TiO_2 (1:100, 1:20, 1:10, 1:1) (Fig. 4A) show mass loss at around 740, 790, 800, and 910ºC, respectively. It was attributed to the C_{60} decomposition on the basis of the increased mass loss with the increasing mass ratios of C_{60} to the TiO_2. In those temperature ranges DSC endothermic peaks appeared too (Fig. 4B). The higher amount of fullerene was applies in C_{60}/TiO_2 composites, the greater heat flow was released. Therefore, both TGA and DSC curves confirm the appropriate mass ratios of C_{60} to TiO_2 as they were introduced during synthesis. Besides, the small endothermic peaks at 730, 800, 820, and the curve bend at 920ºC on the curves of C_{60}/TiO_2 (1:100, 1:20, 1:10, 1:1, respectively) can be attributed to the polymorphic anatase-rutile transformation [40].

Fig. 5 shows the UV-VIS diffuse-reflectance spectra of TiO_2 and prepared C_{60}/TiO_2 composites. It was found that TiO_2 exhibits only one absorption band edge, while C_{60}/TiO_2 displayed two absorption band edges. The band gap energies of the samples were estimated using the following equation: $E_g = 1240/\lambda$, where E_g is the band gap energy (eV) and λ is the absorption wavelength (nm). The first E_g for TiO_2 and C_{60}/TiO_2 (1:100; 1:20; 1:10; 1:1) was determined to be 3.14 eV, 3,06 eV, 2.99 eV, 2.95 eV and 2.25 eV, respectively. The emergence of the second band edge for all C_{60}/TiO_2 composites indicates that C_{60} doping had occurred. The results suggest that C_{60}/TiO_2 composites have the possibility of higher photocatalytic activity under solar light irradiation.

Photocatalytic Activity Studies

The photodegradation of methylene blue (MB) was measured in order to probe how coupling C_{60} to TiO_2 affects photocatalysis. Fig. 6 shows the MB absorption spectra during the photodegradation reaction. A steady decrease of the absorbance of the methylene blue solution was

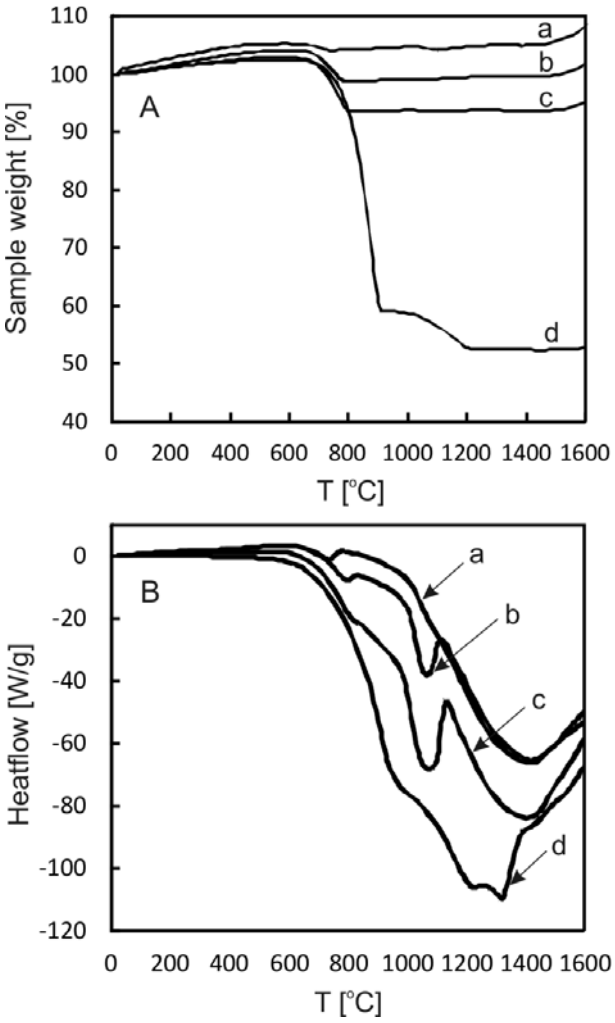

Fig. 4. Thermal analysis profile of C_{60}/TiO_2 composites with mass ratios of 1:100 (a), 1:20 (b), 1:10 (c), and 1:1 (d): TGA (A), DSC (B).

observed in the experimental time. The disappearing peaks at 244, 290, 610, and 662 nm in the UV-VIS-spectra indicate a degradation of the MB molecules. However, above 230 nm, where the isosbestic point has occurred, a small increase in absorbance values was observed. These observations suggest that the photochemical reduction of MB has taken place. According to previously published reports [41, 42], the observed photobleaching and the increase of the peak at 230 nm corresponds to the generation of leucomethylene blue, which main absorption peak is at this wavelength. The presented conclusion was confirmed by chromatographic analysis. The obtained results proved that phodegradation of MB is a more complex process and at least four intermediates were detected after a 30-minute reaction. The recorded chromatograms showed five peaks at retention times 2.01, 3.38, 5.14, 6.49, and 9.33 min, which correspond to MB and its photoproducts, respectively. The same number of peaks at the same retention times were present in all chromatograms, no matter the mass ratio of C_{60} to the TiO_2 in the applied photocatalysts. Those observations indicate that the mechanism of the MB degradation is the same in the case of the application of all composites. The only difference concerns the speed rate of the MB decomposition. It was observed that some generated photoproducts are light-sensitive and disappeared during irradiation [41, 42]. These results suggest that the presence of C_{60} on TiO_2 surface enhances photocatalytic activity of TiO_2 by its sensitization. C_{60} fullerene is easily transformed by UV/VIS radiation into a single excited state that is rapidly converted into the much longer-lived triplet excited state [43]. $^{3*}C_{60}$ exhibits the ability to accept up to six electrons [44].

The energy levels of the C_{60} LUMO orbital and TiO_2 conduction band are equal to -4.1 eV [45] and -4.26 eV [46], respectively. The difference in these values causes an electron transfer from C_{60} to titania conduction band. The electron injected to the TiO_2 leads to the creation of radicals, which are responsible for degradation of organic matter [35]. The obtained results showed that anchoring fullerene on TiO_2 surface by evaporation-drying method improves its photocatalytic property.

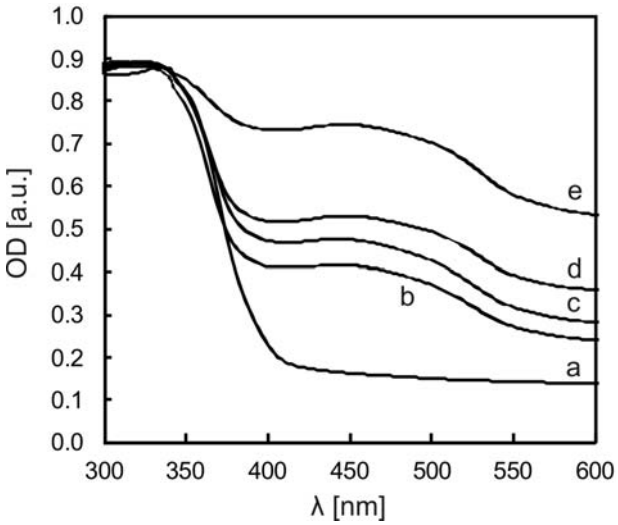

Fig. 5. UV-VIS diffuse-reflectance spectra of TiO_2 (a) and prepared C_{60}/TiO_2 in mass ratios of 1:100 (b), 1:20 (c), 1:10 (d) and 1:1 (e).

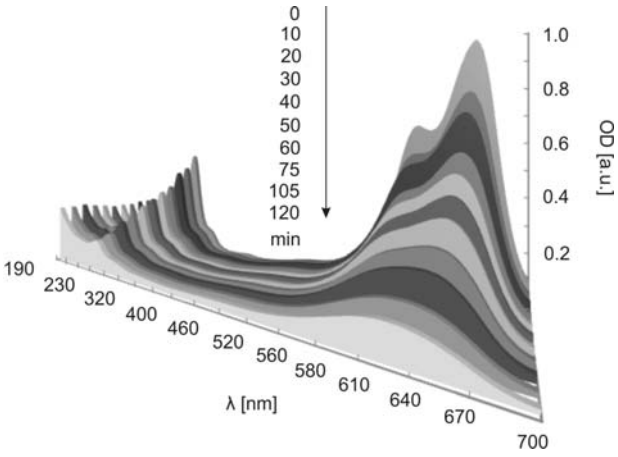

Fig. 6. Normalized UV-VIS spectra of MB with the increasing irradiation time during application of C_{60}/TiO_2 (1:20) as a photocatalyst.

Table 1. Apparent kinetic constant (k_{app}) and half-time of pristine TiO_2 and C_{60}/TiO_2 composites.

Catalyst	k_{app} [mol/L]	$t_{1/2}$ [min]
TiO_2	0.0057	122
C_{60}/TiO_2 (1:100)	0.0101	69
C_{60}/TiO_2 (1:20)	0.0117	59
C_{60}/TiO_2 (1:10)	0.0099	70
C_{60}/TiO_2 (1:1)	-	-

Results of kinetic studies are presented in Table 1. The plot of $\ln(C_o/C_t)$ versus t (Fig. 7) was used for the estimation of the pseudo first-order rate constant, k_{app}, and the half-life, $t_{1/2}$, of the MB photocatalytic degradation. The photocatalysis using the composite of 1:1 mass ratio of C_{60} to TiO_2 was found not to suit pseudo first-order kinetics in the experiment time range. Nevertheless, when a shorter time (20 min) is considered, pseudo first-order kinetics can be observed. The rate of MB degradation in the case of its application was extremely high at the beginning of the process (0-20 min). However, further progress was insignificant. When other composites were introduced as photocatalysts, pseudo first-order kinetics were fulfilled the during whole irradiation process (120 min). The highest $t_{1/2}$ value was obtained when bare TiO_2 was applied, while the lowest in the case of C_{60}/TiO_2 (1:20). It was found that the greater amount of C_{60} was applied the lower k_{app} and higher $t_{1/2}$ values were observed. This relationship worked until 1:10 mass ratio of C_{60} to TiO_2 was reached, because this composite was found to be less photocatalytically active. The highest photocatalytic activity was revealed by C_{60}/TiO_2 (1:20) composite with k_{app} of 0.0117 mol/L and $t_{1/2}$ of 59 min.

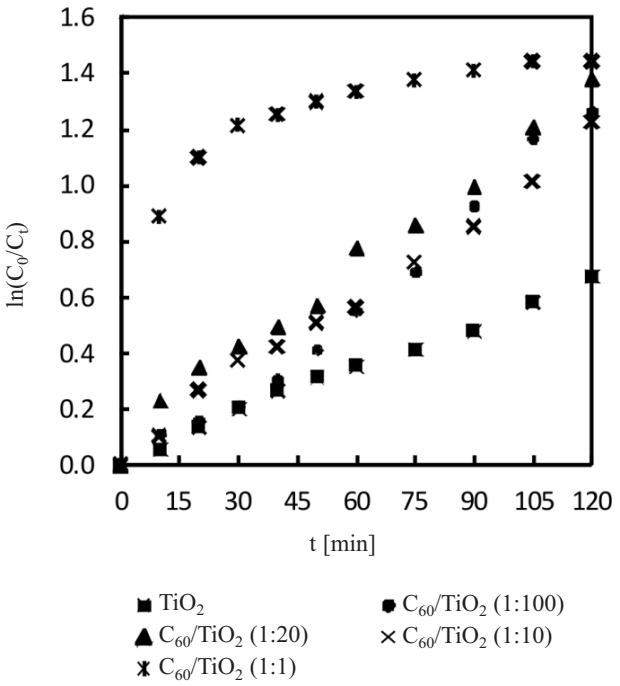

Fig. 7. Relative concentration of MB upon solar simulated light illumination of solutions containing 1.6 mg/mL of the TiO_2 or C_{60}/TiO_2 composites of different mass ratios (1:1, 1:10, 1:20, and 1:100).

Higher photocatalytic activity of prepared nanocomposites can be undoubtedly attributed to the C_{60} presence. We believe that that enhancement results from the absorptivity of C_{60} and the sensitization of the TiO_2. Therefore, when solar energy is applied not only ultraviolet, but also a part of the visible spectrum can be used to observe photocatalytic activity of examined photocatalysts.

Conclusions

Conducted experiments confirmed the photocatalytic ability of C_{60}/TiO_2 nanocomposites. Composites in all prepared mass ratios showed higher catalytic activity than sole TiO_2. However, the best photoactivity was reached in the case of the application of C_{60}/TiO_2 (1:20). We believe that huge potential lies in composites that are based on carbonaceous nanomaterials and TiO_2 as new efficient photocatalysts. As heterogeneous catalysis has been recently applied as a new route for the destruction of undesired compounds present in the environment, prepared nanocomposites could potentially be used during decontamination of organic pollutants. Dyes, to which MB belongs, represent a group of undesired compounds. Investigations concerning the degradation of other representatives of hazardous materials with the usage of described photocatalysts will be shown in a forthcoming paper.

Acknowledgements

This work was financially supported by the National Science Center, Poland (project No. 2012/05/N/ST5/01479).

The authors thank Dr. Marta E. Plonska-Brzezinska and Dr. Anna Basa for taking SEM and TEM images, respectively. DSC, IR spectrometer, and SEM were funded by the EU as part of the Operational Program Development of Eastern Poland 2007-2013, project No. POPW.01.03.00-20-034/09-00.

Author Elżbieta Regulska is a beneficiary of the project "Scholarships for PhD students of Podlaskie Voivodeship." The project is co-financed by European Social Fund, Polish Government and Podlaskie Voivodeship.

References

1. RAJESHWAR K., OSUGI M.E., CHANMANEE W., CHENTHAMARAKSHAN C.R., ZANONI M.V.B., KAJITVICHYANUKUL P., KRISHNAN-AYER R. Heterogeneous photocatalytic treatment of organic dyes in air and aqueous media. J. Photochem. Photobiol. C **9**, 171, **2008**.
2. TAYADE R.J., SUROLIA P.K., KULKARNI R.G., JASRA R.V. Photocatalytic degradation of dyes and organic contaminants in water using nanocrystalline anatase and rutile TiO_2. Sci. Technol. Adv. Mater. **8**, 455, **2007**.

3. KANIOU S., PITARAKIS K., BARLAGIANNI I., POULIOS I. Photocatalytic oxidation of sulfamethazine. Chemosphere **60**, 372, **2005**.
4. JIANG D., XU Y., WU D., SUN Y. Visible-light responsive dye-modified TiO_2 photocatalyst. J. Solid State. Chem. **181**, 593, **2008**.
5. BYRAPPA K., SUBRAMANI A.K., ANANDA S., RAI K.M.L., DINESH R., YOSHIMURA M. Photocatalytic degradation of rhodamine B dye using hydrothermally synthesized ZnO. B. Mater. Sci. **29**, 433, **2006**.
6. REGULSKA E., BRUŚ D.M., KARPIŃSKA J. Photocatalytic Decolourization of Direct Yellow 9 on Titanium and Zinc Oxides. J. Photoenergy **975356**, 1, **2013**.
7. GUARDIA L., VILLAR-RODIL S., PAREDES J.I., ROZADA R., MARTÍNEZ-ALONSO A., TASCÓN J.M.D. UV light exposure of aqueous graphene oxide suspensions to promote their direct reduction, formation of grapheme-metal nanoparticle hybrids and dye degradation. Carbon **50**, 1014, **2012**.
8. BAI S., SHEN X., ZHONG X., LIU Y., ZHU G., XU X., CHEN K. One-pot solvothermal preparation of magnetic reduced graphene oxide-ferrite hybrids for organic dye removal. Carbon **50**, 2337, **2012**.
9. KITSIOU V., FILIPPIDIS N., MANTZAVINOS D., POULIOS I. Heterogeneous and homogeneous photocatalytic degradation of the insecticide imidacloprid in aqueous solutions. Appl. Catal. B-Environ. **86**, 27, **2009**.
10. REGULSKA E., KARPIŃSKA J. Photocatalytic degradation of olanzapine in aqueous and river waters suspension of titanium dioxide. Appl. Catal. B-Environ. **117-118**, 96, **2012**.
11. REGULSKA E., KARPIŃSKA J. Investigation of novel material for effective photodegradation of bezafibrate in aqueous samples. Environ. Sci. Pollut. R. **21**, 5242, **2014**.
12. CHHATZITAKIS A., BERBERIDOU C., PASPALTSIS I., KYRIAKOU G., SKLAVIADIS T., POULIOS I. Photocatalytic degradation and drug activity reduction of Chloramphenicol. Water Res. **42**, 386, **2008**.
13. ZHANG G., CHOI W., KIM S.H., HONG S.B. Selective photocatalytic degradation of aquatic pollutants by titania encapsulated into FAU-type zeolites. J. Hazard. Mater. **188**, 198, **2011**.
14. KARAMANIS D., ÖKTE A.N., VARDOULAKIS E., VAIMAKIS T. Water vapor adsorption and photocatalytic pollutant degradation with TiO_2–sepiolite nanocomposites. Appl. Clay. Sci. **53**, 181, **2011**.
15. HUANG H., LEUNG D.Y.C., LI G., LEUNG M.K.H., FU X. Photocatalytic destruction of air pollutants with vacuum ultraviolet (VUV) irradiation. Catal. Today **175**, 310, **2011**.
16. CHRISTOFORIDIS K.C., LOULOUDI M., MILAEVA E.R., DELIGIANNAKIS Y. Mechanism of catalytic decomposition of pentachlorophenol by a highly recyclable heterogeneous SiO_2–[Fe-porphyrin] catalyst. J. Catal. **270**, 153, **2010**.
17. AMAT A.M., ARQUES A., LÓPEZ F., MIRANDA M.A. Solar photo-catalysis to remove paper mill wastewater pollutants. Sol. Energy. **79**, 393, **2005**.
18. KUWAHARA Y., AOYAMA J., MIYAKUBO K., EGUCHI T., KAMEGAWA T., MORI K., YAMASHITA H. TiO_2 photocatalyst for degradation of organic compounds in water and air supported on highly hydrophobic FAU zeolite: Structural, sorptive, and photocatalytic studies. J. Catal. **285**, 223, **2012**.
19. HALASI G., UGRAI I., SOLYMOSI F. Photocatalytic decomposition of ethanol on TiO_2 modified by N and promoted by metals. J. Catal. **281**, (2), 309, **2011**.
20. SAIEN J., SHAHREZAEI F. Organic Pollutants Removal from Petroleum Refinery Wastewater with Nanotitania Photocatalyst and UV Light Emission. Int. J. Photoenergy **2012**, 1, **2012**.
21. FUJISHIMA A., HONDA K. Electrochemical photolysis of water at a semiconductor electrode. Nature **238**, 37, **1972**.
22. BYRAPPA K., SUBRAMANI A.K., ANANDA S., RAI K.M.L., DINESH R., YOSHIMURA M. Photocatalytic degradation of rhodamine B dye using hydrothermally synthesized ZnO. B. Mater. Sci. **29**, 433, **2006**.
23. GUOA H.X., LIN K.L., ZHENGA Z.S., XIAO F.B., LI S.X. Sulfanilic acid-modified P25 TiO_2 nanoparticles with improved photocatalytic degradation on Congo red under visible light. Dyes Pigments **92**, 1278, **2012**.
24. WANG C., LI J., MELE G., DUAN M.Y., LÜ X.F., PALMISANO L., VASAPOLLO G., ZHANG F.X. The photocatalytic activity of novel, substituted porphyrin/TiO_2-based composites. Dyes Pigments **84**, 183, **2010**.
25. ZHOUA Z.X., QIANB S.P., YAOB S.D., ZHANG Z.Y. Photosensitization of a colloidal TiO_2 semiconductor system with hypocrellin B. Dyes Pigments **51**, 137, **2001**.
26. ZHANG Z., WANG X., LONG J., GU Q., DING Z., FU X. Nitrogen-doped titanium dioxide visible light photocatalyst: Spectroscopic identification of photoactive center. J. Catal. **276**, 201, **2010**.
27. WANG P., ZHOU T., WANG R., LIM T.T. Carbon-sensitized and nitrogen-doped TiO_2 for photocatalytic degradation of sulfanilamide under visible-light irradiation. Water Res. **45**, 5015, **2011**.
28. WANG P., YAP P.S., LIM T.T. C-N-S tridoped TiO_2 for photocatalytic degradation of tetracycline under visible-light irradiation. Appl. Catal. A-Gen. **399**, 252, **2011**.
29. ZHANG J., PAN C., FANG P., WEI J., XIONG R. Mo + C Codoped TiO_2 Using Thermal Oxidation for Enhancing Photocatalytic Activity. ACS Appl. Mater. Interfaces **2**, 1173, **2010**.
30. LEARY R., WESTWOOD A. Carbonaceous nanomaterials for the enhancement of TiO_2 photocatalysis. Carbon **49**, 741, **2011**.
31. MAO C.-C., WENG H.-S. Effect of heat treatment on photocatalytic activity of titania incorporated with carbon black for degradation of methyl orange. Environ. Prog. Sustain. **31**, 306, **2012**.
32. EBRAHIMBEIKI CHIMEH A., MONTAZER M., RASHIDI A. Conductive and photoactive properties of polyethylene terephthalate fabrics treated with nano TiO_2/nano carbon blacks. New Carbon Mater. **28**, 313, **2013**.
33. RAHMAWATI F., WAHYUNINGSIH S., IRIANTI D. The Photocatalytic Activity of SiO_2-TiO_2/Graphite and Its Composite with Silver and Silver oxide. Bull. Chem. React. Eng. Catal. **9**, 45, **2014**.
34. HE Y., ZHANG Y., HUANG H., ZHANG R. Synthesis of titanium dioxide-reduced graphite oxide nanocomposites and their photocatalytic performance. Micro Nano Lett. **8**, 483, **2013**.
35. SELLAPPAN R., SUN J., GALECKAS A., LINDVALL N., YURGENS A., KUZNETSOV A.Y., CHAKAROV D. Influence of graphene synthesizing techniques on the photocatalytic performance of graphene–TiO_2 nanocomposites. Phys. Chem. Chem. Phys. **15**, 15528, **2013**.
36. ZHANG L., DIAO S., NIE Y., YAN K., LIU N., DAI B., XIE Q., REINA A., KONG J., LIU Z. Photocatalytic Patterning and Modification of Graphene. J. Am. Chem. Soc. **133**, 2706, **2011**.

37. MORSELLI D., BONDIOLI F., SANGERMANO M., ROPPOLO I., MESSORI M. Epoxy resins reinforced with TiO_2 generated by nonhydrolytic sol-gel process. J. Appl. Polym. Sci. **131**, 40470, **2014**.
38. HAYLE S.T., GONFA G.G. Synthesis and characterization of titanium oxide nanomaterials using sol-gel method. J. Nanosci. Nanotechno. **2**, 1, **2014**.
39. YAO Y., LI G., CISTON S., LUEPTOW R.M., GRAY K.A. Photoreactive TiO_2/Carbon Nanotube Composites: Synthesis and Reactivity. Environ. Sci. Technol. **42**, 4952, **2008**.
40. YODYINGYONG S., SAE-KUNG C., PANIJPAN B., TRIAMPO W., TRIAMPO D. Physicochemical properties of nanoparticles of nanoparticles titania from alcohol burner calcinations. Bull. Chem. Soc. Ethiopia. **25**, 263, **2011**.
41. SOHRABNEZHAD S.H. Study of catalytic reduction and photodegradation of methylene blue by heterogeneous catalyst. Spectrochim. Acta A **81**, 228, **2011**.
42. MILLS A., WANG J. Photobleaching methylene blue sensitized by TiO_2: an ambiguous system? J. Photochem. Photobiol. A **127**, 123, **1999**.
43. GULDI D.M., PRATO M. Excited-state properties of C_{60} fullerene derivatives. Acc. Chem. Res. **33**, 695, **2000**.
44. APOSTOLOPOULOU V., VAKROS J., KORDULIS CH. LYCOURGHITOS A. Preparation and characterisation of [60] fullerene nanoparticles supported on titania used as a photocatalyst. Colloid. Surface A. **349**, 198, **2009**.
45. SCHULZ G.L., URDANPILLETA M., FITZER R., BRIER E., MENA-OSTERITZ E., BÄUERLE P. Optimization of solution-processed oligothiophene:fullerene based organic solar cells by using solvent additives. Beilstein J. Nanotechnol. **4**, 680, **2013**.
46. CHUNG I., LEE B., He J., CHANG R.P.H., KANATZIDIS M.G. All-solid-state dye-sensitized solar cells with high efficiency. Nature **485**, 486, **2012**.